International Journal of Chemical and Biochemical Sciences
(ISSN 2226-9614)

Journal Home page: www.iscientific.org/Journal.html

Impact of margins on groundwater quality in the province of Taza, Morocco

A. Fiouz [1], M. El Hezzat [2], S. Chakiri [1], A. Najem [3,4], A. Chibani [5], Z. Doudech [6], H. El gasmi [7], I. Warad [8], N. Chahboun [3,9,10], A. Zarrouk [3]*

[1] *Geosciences laboratory, geology department, University Ibn Tofail, Faculty of Sciences, Po.Box. 133, 14000, Kenitra, Morocco*
[2] *Laboratory of Advanced Materials and Process Engineering, Ibn Tofail University, Faculty of Sciences, Kenitra, Morocco*
[3] *Laboratory of Materials, Nanotechnology and Environment, Faculty of Sciences, Mohammed V University in Rabat, P.O. Box. 1014, Rabat, Morocco*
[4] *Institute of Pharmacognosy, Interdisciplinary Excellence Centre, University of Szeged, Szeged, Hungary*
[5] *Nutrition, Health and Environment, Department of Biology, Faculty of Sciences, University Ibn Tofail, Kenitra, Morocco*
[6] *Provincial Public Health Laboratory, Delegation of the Ministry of Health and Social Protection to the Province of Taza, Morocco*
[7] *Ressources Naturelles et Développement Durables, Département Geologie, Faculty of Sciences, University Ibn Tofail, Kenitra, Morocco*
[8] *Department of Chemistry, AN-Najah National University, P.O. Box 7, Nablus, Palestine*
[9] *Laboratory of Natural Resources and Sustainable Development, Faculty of Sciences, Ibn Tofail University, P.O. Box 242, 14000, Kenitra, Morocco*
[10] *Institute of Nursing Professions and Health Techniques, Annex – Kenitra, Morocco*

Abstract

An extensive examination of water derived from six groundwater wells within the Oued Amlil region, Taza province, reveals a profound influence on groundwater quality due to the adjacency of five expansive contemporary olive-pressing mills. Moreover, the presence of retention and evaporation basins for margines serves as a localized source of potential pollution, significantly impacting the quality of the groundwater. The comprehensive analysis underscores heightened levels of specific elements: Polyphenols (3.2 mg/L), electrical conductivity EC (6.8 mS/cm), chemical oxygen demand CDO (96.00 mg O_2/L), chlorides Cl^-(95 mg/L), potassium K^+(99 mg/L), and sodium Na^+(55 mg/L), indicative of margines-induced pollution. To delve into the hydrogeochemical mechanisms underlying groundwater pollution, Principal Component Analysis (PCA) was employed on the physicochemical data of the water samples. This sophisticated statistical methodology unveils significant associations between the pollution levels of the wells, predominantly attributed to margines, and their spatial proximity to the neighboring extensive oil mills. Notably, the outcomes of the physicochemical analyses exhibit discernible increments in pollutant chemical elements downstream of oil mills H1, H2, H3, H4, and H5, highlighting direct wastewater discharge from these industrial facilities into the environment. This aligns with the polyphenol measurements at the S1 control station in the Innaouene River, a tributary of the Oued Amlil aquifer. Furthermore, it becomes evident that pollution levels vary across wells, contingent upon individual well positioning and distance from the pollution source's current draining line. This spatial variance underscores the nuanced impact of proximity on the degree of groundwater contamination in this context.

Keywords: Microbiological parameters, Water quality, Physico-chemical quality, Principal Component Analysis (PCA).

Full length article *Corresponding Author, e-mail: azarrouk@gmail.com

1. Introduction

The olive, an enduring evergreen tree within the Oleaceae family, thrives across a global expanse of 10.8 million hectares spanning 41 countries, particularly prominent in the Mediterranean basin [1]. In the year 2018, worldwide olive cultivation yielded 21.6 million tonnes, with olive oil production reaching 3.2 million tonnes of the world's olive groves, 23% are distributed among major producers such as Spain, Greece, Italy, Portugal, Turkey, Morocco, Syria, and Tunisia. Spain leads as the largest olive oil producer [2]. Morocco boasts widespread olive tree cultivation, spanning various regions excluding coastal and

desert areas. Abundant in locales such as Fès, Boulmane, Taounate, Meknès, Tafilalet, Marrakech, Tensift, Haouz, Beni Mellal, Tadla, Azilal, l'Oriental, Tangier, and Tétouan, the country hosts approximately 550,000 hectares across 400,000 farms. About 200,000 hectares benefit from irrigation, predominantly supporting the production of virgin olive oil. This oil, extracted through mechanical processes from the olive fruit, undergoes a series of treatments encompassing washing, decantation, centrifugation, and filtration [3]. The province of Taza forms a vital pillar of the local agricultural economy, pivoting significantly on olive cultivation. With approximately 89,000 hectares under cultivation, accounting for 74% of the local landscape, the average yield ranges from 1.2 to 2 tons per hectare on non-irrigated land and 2.5 to 3.5 tons per hectare on irrigated land [4]. A discernible upsurge characterizes the trajectory of olive and olive oil production in the province of Taza, notably from 2007 to 2019. In the 2018/2019 period, olive production peaked at 105,000 tons annually, accompanied by olive oil production reaching 10,500 tons annually.

Olive crushing generates large quantities of solid by-products (pomace) and liquid by-products (oil mill wastewater (OMW)), ranging from 1.2 to 1.8 m3 per tonne of olives [5]. The wastewater from oil mills (OMW) has harmful effects on the environment, in particular the pollution of water and soil, which consequently contribute to the disruption of the economic equilibrium of this agro-industrial activity due to the costs associated with their treatment and/or disposal [6]: These are liquid wastes whose complex organic fraction gives them a highly polluting power, in particular the pollution of water and soil, the emission of greenhouse gases, the emission of unpleasant odors and the effect on the development of plants and insects [7]. Analysis of physicochemical parameters has shown that oil mill wastewater is rich in organic matter expressed in terms of BOD and COD, and contains 4.2 g/l of total sugars and 7.8 g/l of total polyphenols, with an acid pH assessed at 4.6 [8]. However, when it comes to the treatment of wastewater from oil mills (OMW), the situation is more difficult and success is unsatisfactory in the search for an environmentally-friendly and economically feasible treatment method. While 0.4 to 0.6 m3 of the wastewater is produced per tonne of product in the pressing process, in three-phase systems the wastewater generated is estimated to be 1.1 to 1.5 times the weight of crushed olives [9], and in two-phase systems, the average volume of wastewater is 0.2 m^3/tonne [10]. As this system does not require much dilution water and improves the oil yield of the process, it is compulsory either to spread the 60%-moisture pomace in the olive groves, with the problems that can arise from the presence of polyphenols (a very poorly biodegradable product), which can asphyxiate the soi or to use dryers to recover the fresh pomace [11].

In this study, we focused on the impact of the wastewater from oil mills (OMW) on groundwater quality in the Oued Amlil aquifer in the province of Taza, suspected to be caused by the ever-growing olive industry. To this end, seven (7) stations were selected for the physico-chemical study: 6 sampling stations in groundwater wells, and 1 water sampling station in the river, reflecting the probable contribution of margines released by the largest oil mills located in our study area during the olive crushing period.

2. Materials and methods

Study area

The Oued Amlil is situated as the central hub within a village, positioned approximately 30 kilometers west of Taza city along national road no. 6. This village falls within the jurisdiction of the Taza province (Figure 1). Nestled within a sub-catchment of the Innaouene watershed, its geographical scope spans from 290 meters downstream to 1169 meters upstream, encompassing an area of 153.7 square kilometers.

The climatic conditions in this region are defined by two distinct seasons: an extensive rainy period spanning nearly 8 months from October to May, yielding an average rainfall of approximately 580 millimeters (with mountainous areas experiencing notably higher rainfall, up to 1,500 millimeters). Following this, a dry season prevails from June to September, marked by average maximum temperatures nearing 35°C. Notably, the Oued Amlil watershed boasts a landscape typified by steep slopes (53% of the watershed exhibiting steep to extreme inclines) and sparse vegetation cover, with 13.3% of the total watershed area predominantly occupied by 74% olive trees (Figure 2).

The predominant lithological formations primarily consist of marly, soft, and impermeable structures, accounting for approximately 71.5%. This composition significantly influences the drainage density, which measures approximately 3.83 km-1 (km/km^2), indicative of the lithological composition favoring surface runoff due to its impermeable nature. Consequently, the hydrographic network, characterized as orders 6, exhibits heightened activity during periods of intense and concentrated rainfall [12].

Geological and hydrogeological setting

The water table of Oued Amlil is situated above the Liassic aquifer, part of the Fès-Taza corridor, encompassing an expansive area of 1,500 km^2. Comprised of Middle Lias dolomites and Upper Lias limestones, it serves as an extension toward the east of the profound nappe within the Fès-Meknès basin [13]. Its northern reach spans across the Sebou plain, extending eastward from Sidi Hrazem and following the left bank of the Innaouène river until the Touaher pass. To the south, its coverage includes the Ghomra and Matmata basins, the downstream Sebou gorges after Ain Sebou, and the northern sector of the Middle-Atlasic limestone plateau [14]. Its demarcations are defined by the Sud-Rifain fault in the north, the boundaries of schistose basement outcrops to the south and east, and the Sidi Hrazem fault system to the west [15].

Distinct geological formations contribute to this aquifer system, including Paleozoic outcrops within the Tazekka massif and the punctuated presence of Middle-Atlasic limestone plateau. These formations comprise schists intermittently intersected by quartzite beds and siliceous veins (Figure 3). The Permo-Triassic outcrops border the Paleozoic basement, characterized by dolerite intercalations within two clay series. Dolerite thickness ranges from 100 to 200 meters, while the lower clay series measures 50 to 100 meters and the upper series, 0 to 20 meters. These formations occasionally exhibit gypsum and/or saline properties [16].

Two distinguishable formations exist within this complex structure: the Lower Lias, dominated by dolomites, and the Middle Lias, primarily characterized by coarse-bedded oolitic limestone. These formations are separated by a layer of red and/or chocolate clays, varying between 10 to 20 meters in thickness. While the Lower Lias prominently lines the Atlas rim and transitions to Miocene marl, the Middle Lias outcrops within the Oued Zereg syncline between Oued Kaouane and Oued Amlil. These formations possess significant outcrop areas and triple porosity (fissural, karstic, and/or interstitial).

In the phreatic aquifer of the marly overburden within the Fès-Taza corridor, specifically at our study site, the water level oscillates between 10 to 20 meters above ground level. Wells rarely exceed a depth of 35 meters in this context.

Sampling and analysis methods

Collecting water samples is a critical process requiring meticulous care to prevent contamination and ensure the homogeneity of samples, maintaining their physicochemical characteristics. The accuracy of analytical results and their subsequent interpretation is significantly influenced by the method of sample collection and handling:

Clean containers are used for water samples, meticulously rinsed multiple times with the specific water to be analyzed. Subsequently, these containers are hermetically sealed to eliminate any air bubbles within the bottle. Each container is clearly marked with the corresponding sampling site number, while comprehensive records of the sampling date and location are meticulously logged onto a designated card.

Following AFNOR standards outlined by Rodier (RODIER, 2009) (Bahroun et al., 2016), water samples, obtained in 1-liter glass bottles, are promptly transported in coolers and stored at a temperature of 4°C.

For this study, six wells (P1, P2, P3, P4, P5, and P6) and a control water point (S) positioned hydraulically upstream at the Innaouene River level were specifically chosen. These sites were selected to examine the potential impact of olive oil discharges on the groundwater's physicochemical quality. The strategic positioning of these wells in proximity to the region's major industrial oil mills and the storage and evaporation basins for oil mill wastewater (OMW) is graphically represented in Figure 4.

- Well P1 is situated in close proximity to oil mills H1, H2, and H3.
- Well P3 is located adjacent to oil mill H4, while P2 lies between oil mills H4 and H1.
- Wells P4, P5, and P6 are strategically positioned near oil mills H4, H5, and H6, respectively.

The sampling campaign was conducted during the olive-growing season of 2022, allowing for the comprehensive assessment of potential influences on groundwater quality stemming from olive oil-related activities. With The physicochemical analysis of groundwater samples obtained from the Oued Amlil aquifer was conducted following standardized methodologies. On-site measurements of temperature (T°C), hydrogen potential (pH), electrical conductivity (EC), and dissolved oxygen (O_2) were carried out using a portable Multiparameter HD98569.

Laboratory analysis involved assessing factors indicative of mineral pollution: volumetric analysis for bicarbonate ion (HCO_3^-), chlorides (Cl^-), calcium (Ca^{2+}), and magnesium (Mg^{2+}); molecular absorption spectrophotometry for sulfates (SO_4^{2-}), ammonium ions (NH_4^+), nitrite ions (NO_3^-), and orthophosphates (PO_4^{3-}); and flame spectrophotometry for sodium (Na^+) and potassium (K^+). The prescribed analytical methods adhered to recommendations by Rodier [17] Calcium (Ca^{2+}), sodium (Na^+), and potassium (K^+) levels were determined using a flame emission photometer according to [18]. To extract phenolic compounds, contaminated wastewater samples from oil mills (OMW) underwent a specific process. Initially, these samples were stored at -20°C, thawed at 4°C, acidified to pH = 2, and subjected to three hexane washes to eliminate the lipid fraction. The subsequent extraction method, based on [19], utilized ethyl acetate as the solvent due to its high efficiency in extracting phenolic compounds. The ethyl acetate extraction process involved multiple steps of vigorous mixing, centrifugation, and evaporation under vacuum, resulting in a dry residue dissolved in methanol for quantification.

Quantification of phenolic compounds relied on spectrophotometric analysis using the Folin-Ciocalteu method described by [20]. This method involves the reduction of a yellow reagent (Folin-Ciocalteu reagent) to a blue complex upon oxidation of polyphenols, with the intensity of the color directly proportional to the levels of oxidized phenolic compounds. For analysis, 1 ml of each extract was combined with 5 ml of diluted Folin-Ciocalteu reagent and 4 mL of sodium carbonate solution, homogenized, and incubated in darkness at room temperature for 2 hours. Subsequently, spectrophotometric measurements were conducted at 765 nm [21]. Calibration curves were prepared using gallic acid as the standard, and results were expressed in milligrams of gallic acid equivalent per milliliter of water (mg EAG/mL).

A standard gallic acid solution was prepared by dissolving 10 mg of gallic acid in 100 mL of methanol to achieve a concentration of 0.2 mg/mL.

Statistical analysis

The study employed Principal Component Analysis (PCA) to investigate potential correlations between the distribution of oil mill wastewater (OMW) and wells exhibiting elevated phenolic concentrations. Statistical analysis was conducted using STATISTICA Version 10 software, focusing on six samples and 18 variables for thorough examination. PCA is a powerful tool in identifying underlying patterns and relationships within complex datasets, aiding in the understanding of potential associations between specific variables and sample locations.

3. Results and Discussions

Control The unregulated discharge of excessive volumes of oil mill wastewater (OMW) from modern and semi-modern oil mills, especially when evaporation basins are insufficient, poses significant environmental hazards. This untreated discharge directly into the environment leads to severe environmental repercussions.

The infiltration of even minute amounts of phenolic compounds can significantly impact groundwater quality [22]. The concentrations of polyphenols present in the wastewater from oil mills (OMW) alone pose a substantial risk for groundwater pollution, particularly after discharges into rivers. These water bodies serve as conducive environments for direct groundwater recharge, amplifying the potential for contamination.

An essential step in evaluating the extent of pollution by this particular type of pollutant necessitated an analysis of the polyphenol content within the well water of the Oued Amlil region. This analysis aimed to gauge the level of contamination caused by such pollutants in the groundwater, specifically assessing the presence and degree of polyphenol contamination resulting from oil mill wastewater discharges.

Table 2 presents a comprehensive statistical analysis of physicochemical parameters found in groundwater samples sourced from the Oued Amlil region.

An examination of dissolved polyphenol levels in control samples, acquired from station S1 along the Innaouene River situated hydraulically upstream of the wells selected for this study, revealed a notably high value of 33.86 mg/L during the olive-pressing season. This observation underscores the discharge of substantial surplus wastewater from oil mills (OMW), which the evaporation basins cannot adequately manage, thereby unable to handle the entirety of the liquid waste generated by neighboring oil mills.

The wastewater from oil mills, laden with polyphenols, emerges as a significant potential source of groundwater pollution. Analysis specifically targeting dissolved polyphenols in water samples indicates contamination in wells P2, P3, P4, P5, and P6. Conversely, well P1 shows no contamination, registering a value of zero. The average recorded across these contaminated wells stands at 1.73 mg/l ± 1.24. These findings reveal that the water extracted from these wells contains levels of polyphenols well above the established Moroccan drinking water standard, set at 0.01 mg/l [23].

Based on the previous table 2, In the Oued Amlil region, groundwater temperatures range consistently from 19°C to 20.7°C, averaging 19.85°C ± 0.83. These temperatures fall below the World Health Organization's (WHO) recommended guide value of 25°C [24], which underscores the importance of considering climatic conditions when assessing water intended for human consumption.

Regarding acidity and alkalinity, most of the sampled waters exhibit slightly acidic to alkaline pH values, ranging between 6.87 and 7.15, with an average of 6.87 ± 0.20.

Measured conductivities (EC) span from 2.27 mS/cm to 6.8 mS/cm, averaging 4.94 ± 1.67 mS/cm. These values surpass the WHO's recommended drinking water standard of 0.40 mS/cm.

Nitrogen is predominantly present in the form of nitrate (NO_3^-), with values ranging from 7.00 to 21.00 mg/L, averaging 14.87 ± 5.76 mg/L. These values remain well below the WHO standard of 50 mg/L.

Sulfate (SO_4^{2-}) concentrations range from 35 to 41 mg/L, averaging 37.67 ± 2.15 mg/L.

Chloride (Cl^-) levels vary from 37 mg/L to 95 mg/L, averaging 65.25 ± 22.87 mg/L. These concentrations remain below the WHO standard of 200 mg/L.

Bicarbonates (HCO_3^-) exhibit a wide variability, ranging from 260 mg/L to 650 mg/L, with an average of 491.67 mg/L. The order of abundance for anions is $HCO_3^- > Cl^- > SO_4^{2-} > NO_3^-$.

Calcium (Ca^{2+}) concentrations fluctuate from 65.00 mg/L to 110.00 mg/L, averaging 65.25 ± 16.57 mg/L. In wells P3, P4, and P6, this surpasses WHO potability standards. Concerning Magnesium (Mg^{2+}), only well P4 exceeds the drinking water standard.

The chemical composition of water is intricately tied to the geological formations it traverses and the soil characteristics it encounters. To decipher this, the collected data underwent hydro-chemical analysis. Diagramme software (version 6.75) was instrumental in chemically classifying the water. It facilitated the graphical representation of major cations (Ca^{2+}, Mg^{2+}, Na^+, and K^+) and major anions (HCO_3^-, Cl^-, SO_4^{2-} and NO_3^-) within both the Piper triangular diagram and the Schöeller-Berkaloff diagram.

These diagrams, namely the Schöeller-Berkaloff and Piper diagrams, serve as powerful tools in characterizing the chemical facies of water. They offer concise visualizations of analytical results, enabling easy characterization of waters, monitoring their evolution, and facilitating comparisons with other mineral waters exhibiting similar physicochemical compositions. This graphical representation provides a swift and comprehensive overview of the water's chemical makeup, aiding in its detailed characterization and analysis.

Piper diagram

The Piper diagram, depicted in Figure 6, serves as a tool to visually depict the chemical facies present in a collection of water samples. Comprising two triangles symbolizing cationic and anionic facies, along with a rhombus representing a comprehensive synthesis of the overall facies.

This diagram is instrumental in various aspects: Illustrating Chemical Evolution and Mixtures: It effectively illustrates the chemical evolution of water over time and can elucidate mixtures resulting from blending waters with differing mineral compositions. Inferring Geological Nature: By analysing chemical analyses, it aids in establishing correlations between water chemistry and the lithological nature of the rocks through which the water passes. This correlation provides insights into the geological characteristics of the area.

Comparative Analysis and Spatial Tracking: By projecting multiple samples simultaneously, it enables the tracking of their evolution across both time and space. This comparative approach helps in assessing variations, identifying mixing patterns, and comprehending the concept of physicochemical property changes across different locations and periods.

In essence, the Piper diagram is a versatile tool that not only visually represents the chemical characteristics of water samples but also facilitates the analysis of their evolution, comparison, and their relationship with geological

formations, offering a comprehensive understanding of water chemistry in various contexts.

Schoeller Berkaloff diagram

The Schöeller-Berkaloff diagram, as shown in Figure 7, serves as a method to depict the chemical facies of multiple water samples. Each sample is represented by a broken line, with the concentration of individual chemical elements depicted by vertical lines on a logarithmic scale. The broken line connecting these points illustrates the chemical composition across different elements for each sample.

From the analysis conducted, it can be concluded that the chemical facies observed in all six wells analyzed exhibit a consistent pattern of calcic and magnesian bicarbonate. This uniformity across samples suggests a predominant influence from the dissolution and leaching processes of Middle Lias dolomites and Upper Lias limestones. These geological formations appear to significantly impact the chemical composition of the water, resulting in consistent calcic and magnesian bicarbonate facies across all analyzed samples.

Piezometric map

The measurement campaign for piezometric water levels conducted in April 2021, combined with data from the Water Resource Inventory (IRE) gathered by Sebou water basin management, has resulted in the creation of a piezometric map showcasing the water table. The primary objective of this map is to enhance our comprehension of the aquifer's piezometry. This comprehensive visualization has allowed us to map existing flow directions and identify the recharge zones corresponding to wells P2, P3, P4, P5, and P6, which were specifically selected for analysis (Figure 8). This mapping exercise provides crucial insights into the aquifer's dynamics, highlighting the flow patterns and key areas responsible for recharging the selected wells.

The piezometric map depicted above was constructed utilizing Surfer software (Version 16.6.484) and relies on on-site piezometric measurements. The critical aspect we focus on in this map pertains to the direction of groundwater flow. Understanding this flow pattern is particularly pertinent as it correlates with the movement and transfer of key chemical pollutants found in oil mill wastewater (OMW), notably polyphenols. This significance is underscored by the elevated polyphenol levels detected at station S1, emphasizing the relevance of comprehending groundwater flow directions in tracing the movement of these pollutants within the aquifer system.

Principal Component Analysis

Principal Component Analysis (PCA) is a robust statistical technique employed to condense and compare complex information across systems. It serves to elucidate chemical similarities among diverse water sources or mineral acquisition points, elucidating the underlying variables that govern these processes. PCA's strength lies in its ability to handle a vast array of variables and samples simultaneously. This method is extensively utilized for interpreting hydro-chemical data due to its effectiveness [25,26].

In this specific study, PCA was executed on a data matrix comprising 18 rows, representing wells (P1, P2, P3, P4, P5, and P6), and 6 columns, representing the measured or analyzed physicochemical variables. The resulting correlation coefficients between the various elements are tabulated in Table 3. This matrix of correlation coefficients serves to reveal the relationships and interdependencies among the different variables, aiding in the comprehensive understanding of the hydro-chemical dataset and its underlying dynamics. The eigenvalues derived from the correlation matrix provide insights into the percentage of variance explained by each factor, as indicated in Table 3. The initial factorial design, encompassing axes F1 and F2, elucidates 88.64% of the total inertia. Table 4 delineates the first five factors along with their corresponding eigenvalues and expressed percentages. It's evident that these five factors collectively encapsulate 100% of the information, with 88.64% attributed to factor 1 and 7.87% to factor 2. Notably, the first two factors cumulatively represent 96.51% of the total variance. The combined information represented by the F1-F2 pair alone surpasses 96.51%, suggesting that these two factors encapsulate most of the information concerning the mechanisms governing the chemical evolution of the region's waters.

Given these percentages, it's reasonable to focus the analysis solely on these two factors since the cumulative total variance should ideally exceed 70% for a valid PCA of a region. The eigenvectors, defining each of these factors in relation to the variables, are outlined in Table 5. These vectors provide crucial insights into the variables' relationships and contributions to the identified factors, aiding in a deeper understanding of the mechanisms controlling the chemical evolution of the water sources in the region. The analysis of the PCA results reveals distinctive patterns across the F1 and F2 axes, shedding light on their contributions to the dataset. The F1 axis, capturing 88.64% of the inertia, demonstrates a contrasting relationship. It positively correlates pH and dissolved oxygen O2 while exhibiting a negative association with phenolic (PPH), organic and mineral compounds (CDO, HCO_3^-, Cl^-, NO_2^-, NO_3^-, Na^+, K^+, Mg^{2+}, Ca^{2+}, CE, SAL), indicating their strong contribution on the negative side of this axis. On the other hand, the F2 axis, which accounts for 7.88% of the inertia, showcases a different set of opposing relationships. It contrasts temperature, NH_4^+ , PO_4^{3-}, and NO_2^- ions with SO_4^{2-} and NO_3^- ions ions, attributing negative contributions to the expression of this axis.

Utilizing the hierarchical classification based on the physicochemical water quality of the wells, the analysis discerned four distinct groups of stations, depicted in Figures 9 and 10. These groupings likely signify specific clusters or categories within the dataset, reflecting unique characteristics or similarities in the physicochemical profiles of the wells. This hierarchical classification provides a structured understanding of the water quality across different well stations, facilitating clearer differentiation and classification based on their shared characteristics.

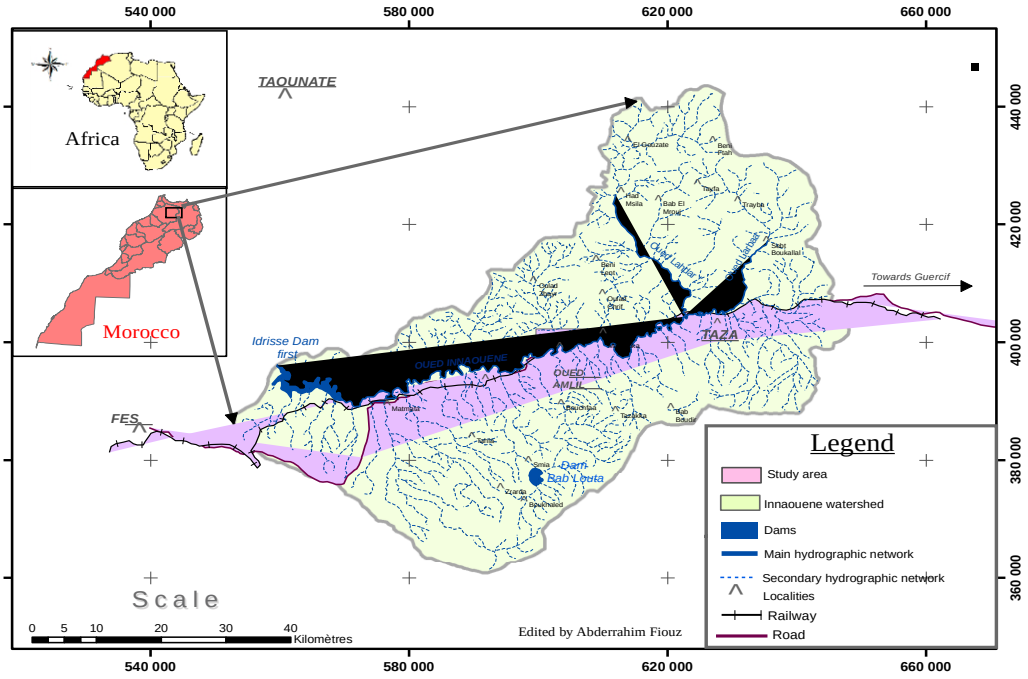

Figure 1: Geographical location of the study area

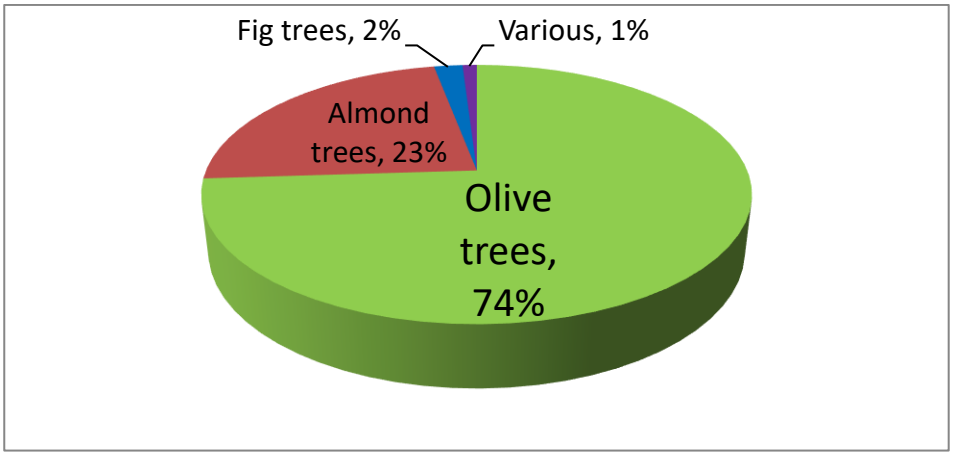

Figure 2: Distribution of fruit trees in the province of Taza

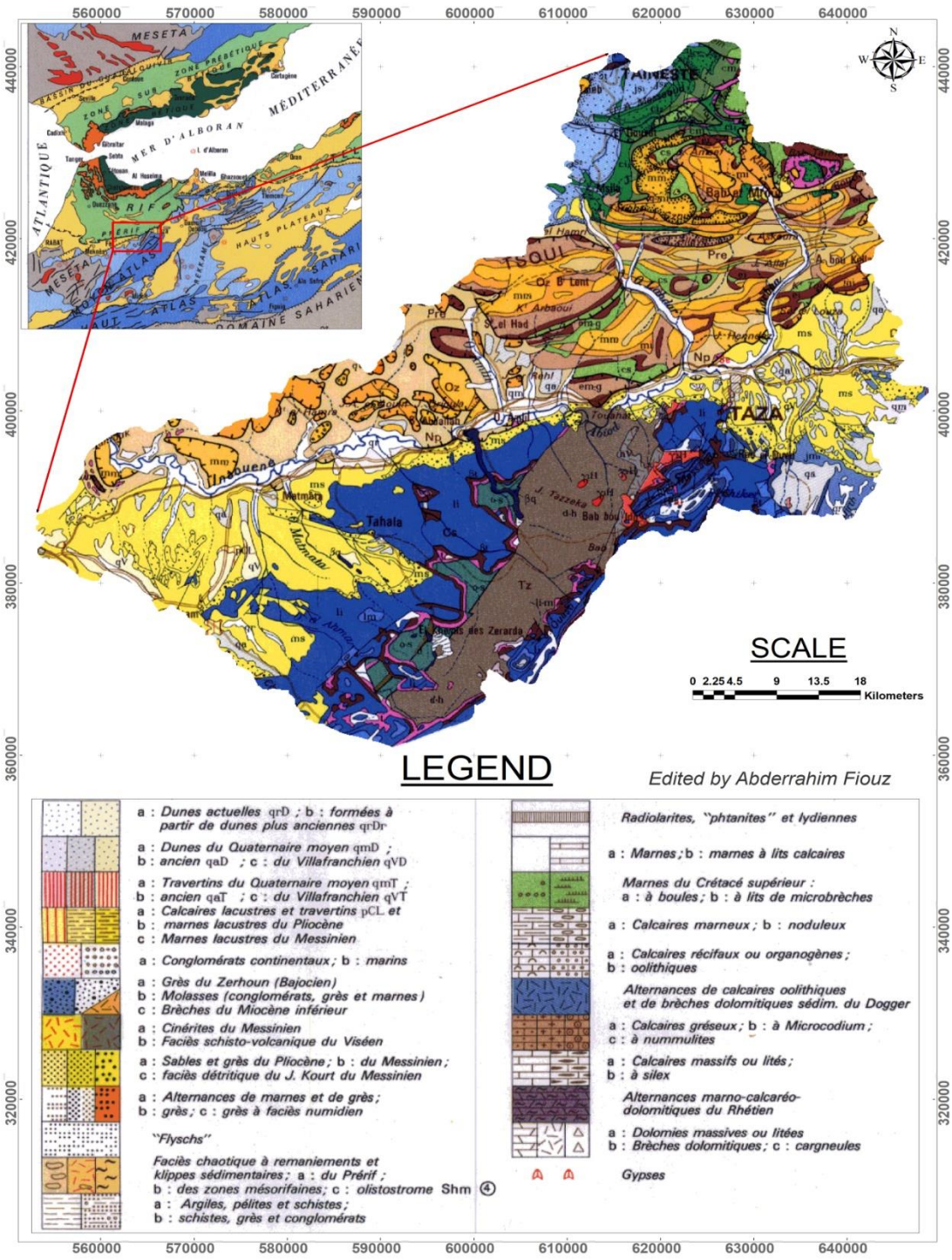

Figure 3: Geological map of the Innaouene watershed, extracted from the 1/500,000 structural map of the Rif.

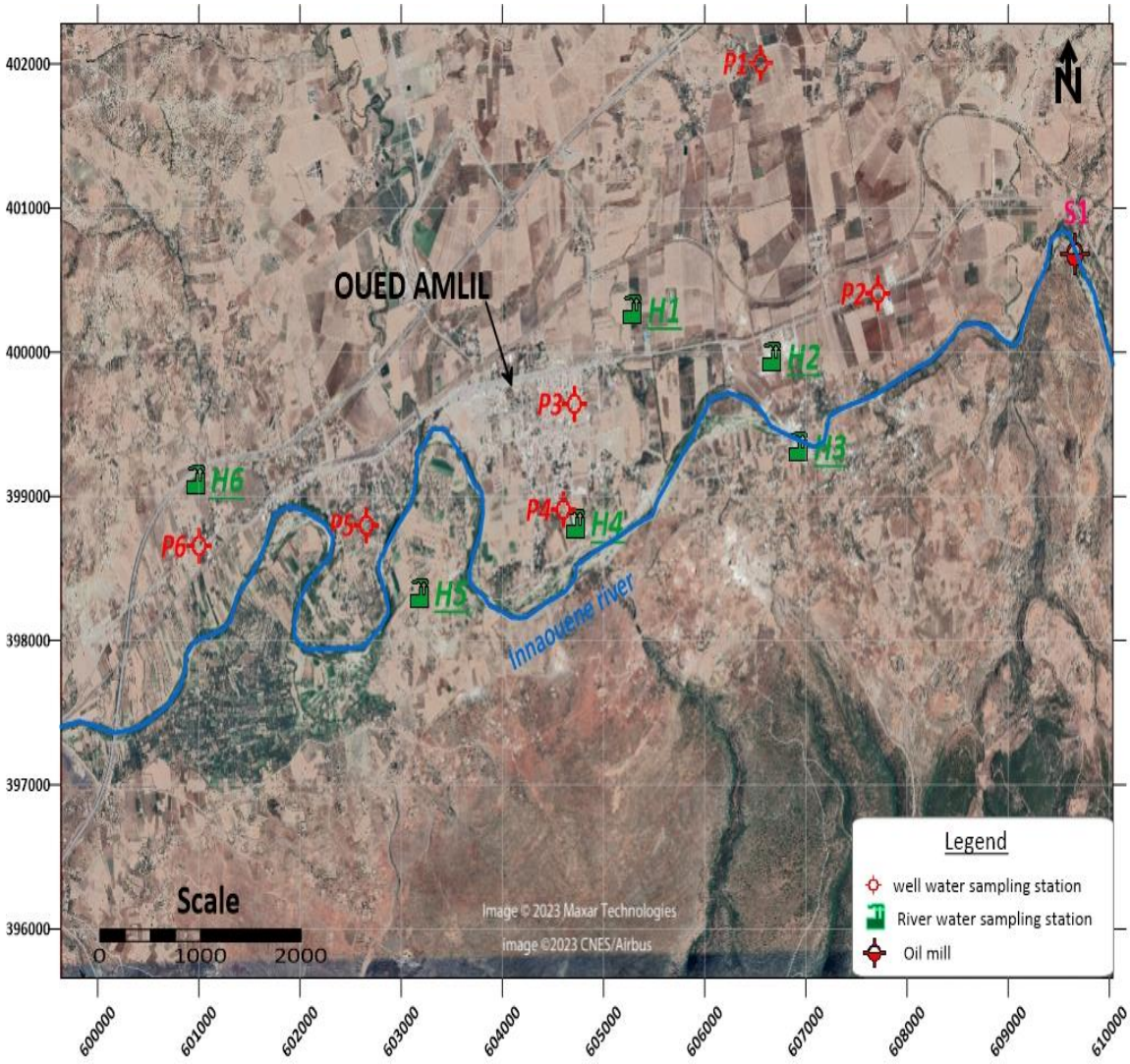

Figure 4: Satellite image showing the location of sampled water points in relation to olive crushing units in the Oued Amlil region.

Table 1: Standard range

Conc (mg/mL)	0	0.125	0.25	0.5	0.75	1	1.2	1.4
Absorbance	0	0.09	0.188	0.451	0.658	0.873	1	1.21

Table 2: Statistical analysis of groundwater physico-chemical parameters.

Settings	Average	Max	Min	Standard deviation	OMS (1994)
T °C	19.85	20.7	19.00	0.83	< 25
PH	6.87	7.15	6.70	0.20	6.5< PH<9.5
O_2	4.47	6.5	3.10	1.21	-
CDO	66.83	96	25.00	30.98	< 400
HCO_3^-	491.67	650	260.00	155.62	-
Cl^-	65.25	95	37.00	22.87	200.00
NO_2^-	2.18	3.2	1.00	0.78	50.00
NO_3^-	14.87	21	7.00	5.76	
PO_4^{3-}	42.68	54	33.00	7.08	-
SO_4^{2-}	37.67	41	35.00	2.15	500.00
Na^+	43.97	55	25.00	11.47	-
NH_4^+	17.19	31	0.22	13.39	-
K^+	70.33	99	27.00	33.19	-
Mg^{2+}	41.58	54	21.00	12.77	50.00
Ca^{2+}	90.67	110	65.00	16.57	100.00
PPH	1.73	3.2	0.00	1.24	-
CE	4.94	6.8	2.27	1.67	-
SAL	1027.67	1500	460.00	373.73	-

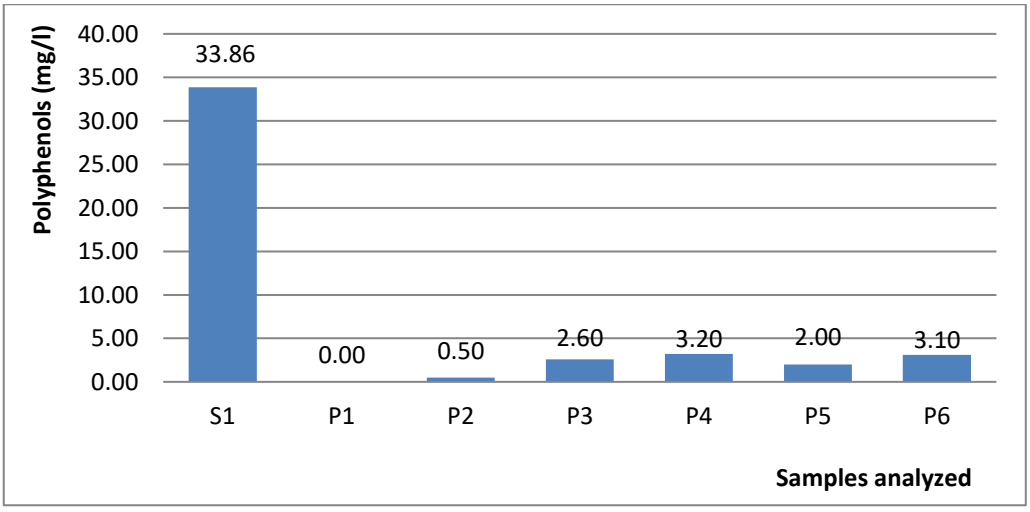

Figure 5: Polyphenol levels in analyzed water samples.

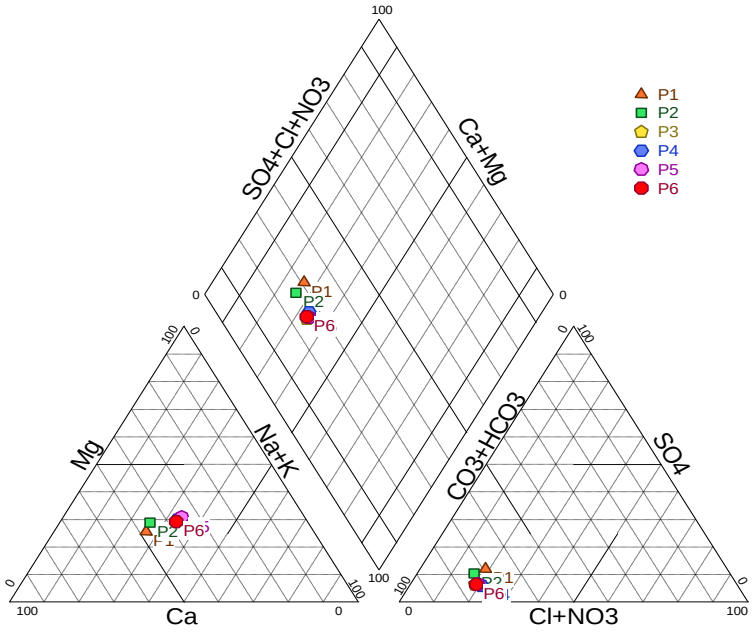

Figure 6: Piper Diagram.

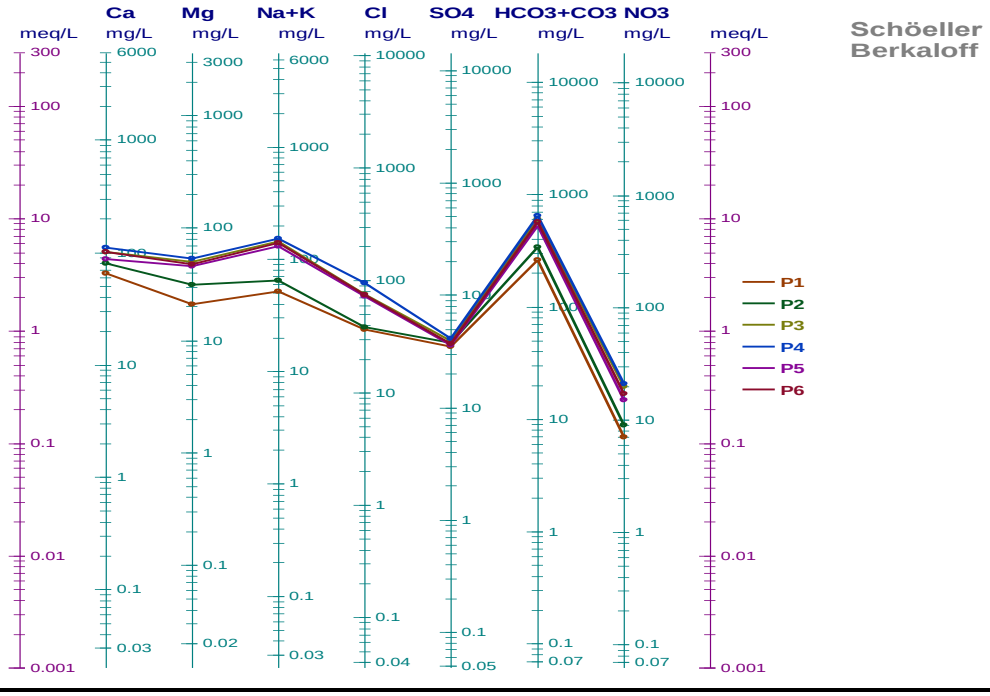

Figure 7: Schöeller-Berkaloff diagram

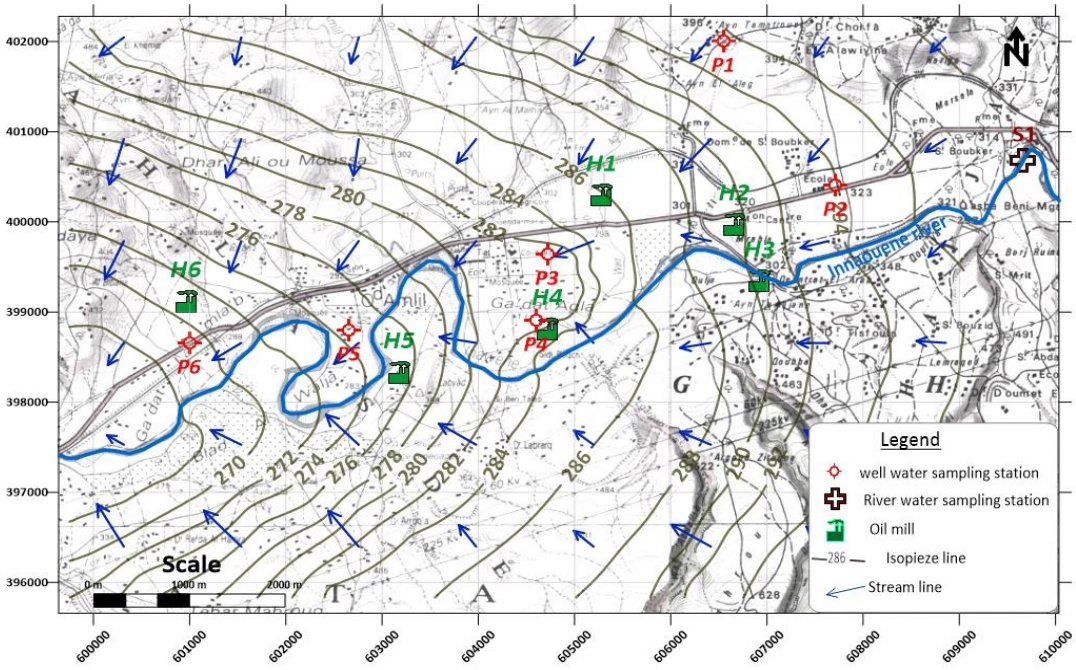

Figure 8: Piezometric map of the water table in the Oued Amlil region

Table 3: Correlation matrix between variables for all stations studied.

	T°c	PH	O2	CDO	HCO3-	Cl-	NO2-	NO3-	PO4--	SO4--	Na+	NH4+	K+	Mg++	Ca++	PPH	CE	SAL
T°c	1	-0.689896	-0.518969	0.723739	0.681918	0.736121	0.514361	0.580909	0.306913	0.223602	0.662155	0.762979	0.720298	0.689403	0.608909	0.658446	0.70479	0.700149
PH	-0.689896	1	0.843648	-0.98861	-0.965515	-0.958364	-0.865008	-0.959898	-0.463574	-0.578887	-0.928295	-0.985411	-0.994606	-0.942142	-0.88318	-0.97614	-0.931095	-0.938129
O2	-0.518969	0.843648	1	-0.897648	-0.949914	-0.897015	-0.990013	-0.951667	-0.822816	-0.873185	-0.971577	-0.872845	-0.879674	-0.96013	-0.970882	-0.916973	-0.965426	-0.964291
CDO	0.723739	-0.98861	-0.897648	1	0.989484	0.977056	0.908023	0.972254	0.551888	0.636257	0.968484	0.995777	0.99757	0.979116	0.918389	0.98738	0.972309	0.975852
HCO3-	0.681918	-0.965515	-0.949914	0.989484	1	0.972768	0.95347	0.988314	0.653272	0.727013	0.991432	0.978437	0.983685	0.994864	0.962627	0.985262	0.992487	0.995157
Cl-	0.736121	-0.958364	-0.897015	0.977056	0.972768	1	0.927279	0.961369	0.647655	0.713722	0.945052	0.986292	0.966736	0.957079	0.924353	0.989627	0.967776	0.967133
NO2-	0.514361	-0.865008	-0.990013	0.908023	0.95347	0.927279	1	0.967015	0.828256	0.895772	0.959694	0.891246	0.890139	0.951913	0.97154	0.94292	0.962959	0.96166
NO3-	0.580909	-0.959898	-0.951667	0.972254	0.988314	0.961369	0.967015	1	0.670273	0.775708	0.972654	0.957198	0.968515	0.973331	0.963636	0.985954	0.971522	0.975916
PO4--	0.306913	-0.463574	-0.822816	0.551888	0.653272	0.647655	0.828256	0.670273	1	0.96008	0.69231	0.542183	0.515883	0.668658	0.794589	0.625118	0.715318	0.704107
SO4--	0.223602	-0.578887	-0.873185	0.636257	0.727013	0.713722	0.895772	0.775708	0.96008	1	0.746235	0.618027	0.608921	0.723736	0.844578	0.721715	0.758782	0.753214
Na+	0.662155	-0.928295	-0.971577	0.968484	0.991432	0.945052	0.959694	0.972654	0.69231	0.746235	1	0.950795	0.958271	0.998559	0.964929	0.959721	0.994861	0.996033
NH4+	0.762979	-0.985411	-0.872845	0.995777	0.978437	0.986292	0.891246	0.957198	0.542183	0.618027	0.950795	1	0.992048	0.965209	0.902038	0.985578	0.963263	0.965503
K+	0.720298	-0.994606	-0.879674	0.99757	0.983685	0.966736	0.890139	0.968515	0.515883	0.608921	0.958271	0.992048	1	0.969364	0.912022	0.980258	0.959964	0.965464
Mg++	0.689403	-0.942142	-0.96013	0.979116	0.994864	0.957079	0.951913	0.973331	0.668658	0.723736	0.998559	0.965209	0.969364	1	0.957544	0.968547	0.996251	0.997332
Ca++	0.608909	-0.88318	-0.970882	0.918389	0.962627	0.924353	0.97154	0.963636	0.794589	0.844578	0.964929	0.902038	0.912022	0.957544	1	0.930609	0.969001	0.971232
PPH	0.658446	-0.97614	-0.916973	0.98738	0.985262	0.989627	0.94292	0.985954	0.625118	0.721715	0.959721	0.985578	0.980258	0.968547	0.930609	1	0.969738	0.971764
CE	0.70479	-0.931095	-0.965426	0.972309	0.992487	0.967776	0.962959	0.971522	0.715318	0.758782	0.994861	0.963263	0.959964	0.996251	0.969001	0.969738	1	0.999546
SAL	0.700149	-0.938129	-0.964291	0.975852	0.995157	0.967133	0.96166	0.975916	0.704107	0.753214	0.996033	0.965503	0.965464	0.997332	0.971232	0.971764	0.999546	1

Table 4: Eigenvalues and percentage of variance expressed.

Value number	Eigenvalue	% Total variance	Cumulative Eigenvalue	Cumulative %
1	15.95575	88.64305	15.95575	88.6431
2	1.4178	7.87668	17.37355	96.5197
3	0.44805	2.48917	17.8216	99.0089
4	0.13378	0.74321	17.95538	99.7521
5	0.04462	0.24789	18	100

Table 5: Eigenvectors (correlation coefficients of reduced-centered variables with factors).

	Factor 1	Factor 2	Factor 3	Factor 4	Factor 5
T °C	-0.678112	0.507093	-0.531254	0.019641	-0.020102
PH	0.947215	-0.2606	-0.163846	-0.073551	0.051154
O_2	0.962674	0.232201	-0.023971	0.131588	-0.038093
CDO	-0.978055	0.194717	0.071606	0.008089	0.017362
HCO_3^-	-0.996038	0.063652	0.047498	-0.038657	-0.010288
Cl^-	-0.978644	0.103259	-0.033459	0.16808	0.047151
NO_2^-	-0.970583	-0.232936	0.047198	0.007595	0.037747
NO_3^-	-0.986583	-0.015939	0.153399	0.028414	-0.045409
PO_4^{3-}	-0.712059	-0.642074	-0.280641	0.042107	0.013473
SO_4^{2-}	-0.774825	-0.620415	-0.01893	0.118089	-0.020674
Na^+	-0.989166	0.003902	0.013632	-0.143772	0.026067
NH_4^+	-0.970024	0.227795	0.020929	0.074878	0.033428
K^+	-0.968217	0.226898	0.098202	0.004886	-0.037494
Mg^{2+}	-0.99129	0.047828	0.007527	-0.116268	0.038482
Ca^{2+}	-0.974236	-0.146728	-0.038277	-0.045414	-0.160645
PPH	-0.984065	0.08307	0.098574	0.114599	0.043182
CE	-0.996037	0.008892	-0.050394	-0.065785	0.03104
SAL	-0.996826	0.018119	-0.031219	-0.070215	0.010197

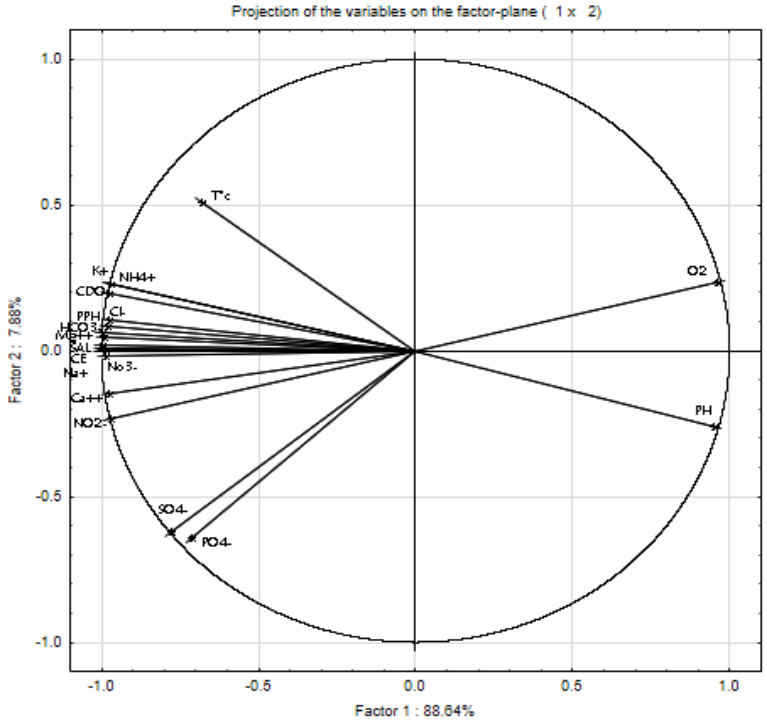

Figure 9: Projection of water physicochemical factors on the plane of the first two axes of Principal Component Analysis.

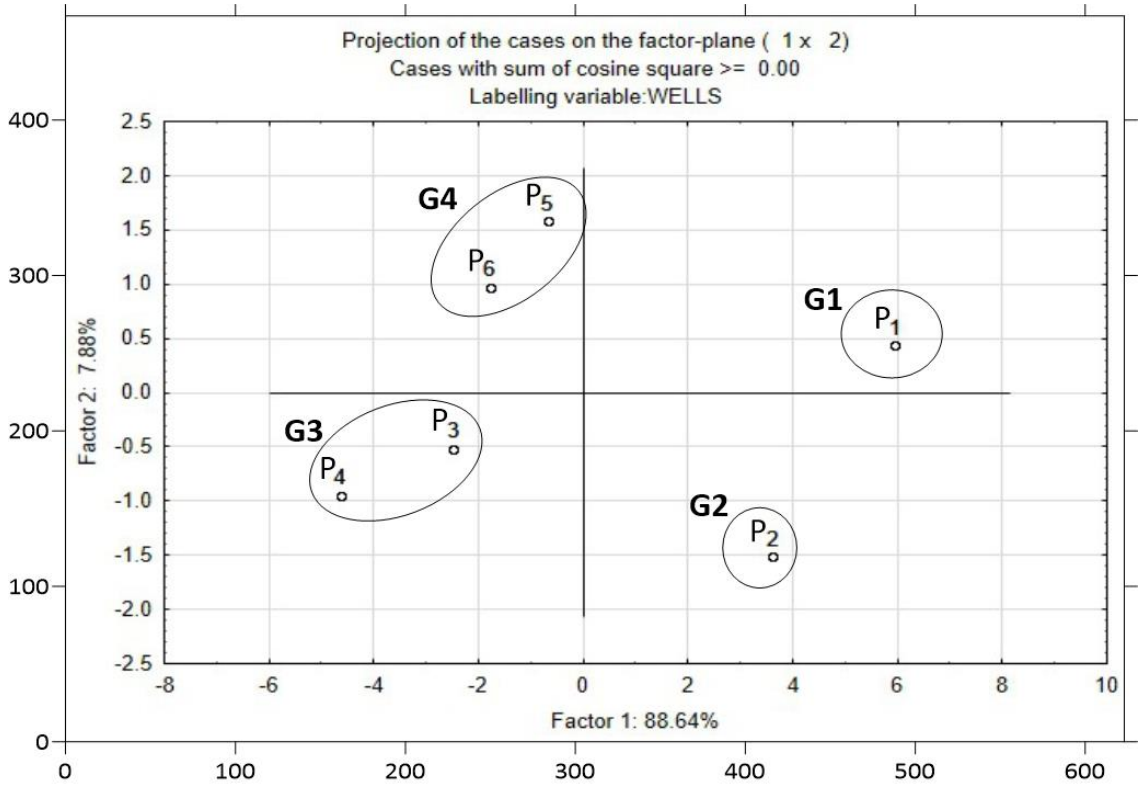

Figure 10: Projection of active observations onto the first factorial plane

Group G1: This group is made up of well P1, located to the north of the three main oil mills H1, H2, and H3, and according to the values of the physicochemical parameters recorded, this well is not polluted by polyphenols.

Group G2: This group is made up of well P2, located to the west of the three main oil mills H1, H2, and H3, and according to the values of the physicochemical parameters recorded, this well shows the beginnings of the wastewater from oil mills (OMW) contamination.

Group G3: This group comprises wells P3 and P4, located close to oil mill H4 and hydraulically downstream of oil mills H1, H2, and H3. They have loaded with elements indicative of wastewater from oil mills (OMW) pollution, namely polyphenols (PPH), K^+, CDO, Cl^-, and Na^+.

Group G4: This group comprises wells P5 and P6, located close to oil mill H5 and hydraulically downstream of oil mill H6 respectively. They are less contaminated than group 3 with elements indicative of the wastewater from oil mills (OMW) pollution.

To summarize the findings of this work, it's clear from this study that the absence The absence of polyphenols in well P1 can be attributed to its advantageous upstream location, shielded from the primary pollution sources of oil mills in the region (H1, H2, and H3).

However, at well P2, positioned westward of the three major oil mills (H1, H2, and H3) and at the hydraulic headwaters, indications of contamination become apparent. This contamination is substantiated by the analysis of control station S1, exhibiting a notably high polyphenol content (33.86 mg/l), which confirms the presence and impact of oil mill wastewater (OMW) from the Innaouene river.

Wells P3 and P4 register heightened levels of indicators signaling OMW pollution. Their proximity to oil mill H4, combined with their hydraulic positioning downstream from oil mills H1, H2, and H3, exposes them to substantial contamination from the oil mill wastewater.

This pollution load consists in particular of polyphenols PPH (P3= 2.60 mg/L and P4=3.20 mg/L), K^+ (P3=93 mg/L and P4=99 mg/L), CDO (P3=87 mg/L and P4=96 mg/L), Cl^- (P3=75 mg/L and P4=95) mg/L, and Na^+ (P3=52 mg/L and P4=55 mg/L).

The piezometric map (Figure 8) serves as confirmation of the contamination observed in wells P3 and P4. The convergence and directional flow lines originating from the Innaouene River and passing through the three oil mills (H1, H2, and H3) provide visual evidence of contamination affecting these wells.

On the other hand, wells P5, situated in proximity to oil mill H5, and P6, located downstream from oil mill H6, display a reduction in the levels of oil mill wastewater (OMW) contamination compared to wells P3 and P4. Despite their hydraulic positioning downstream of the five oil mills (H1, H2, H3, H4, and H5), these wells exhibit lower contamination levels, indicating a regression in the extent of OMW contamination.

The contamination observed in wells P2, P3, P4, and P5 might be attributed not only to the infiltration of water from the Innaouene river but also to the unregulated discharge of wastewater from nearby oil mills. This untreated discharge of oil mill wastewater (OMW) directly into the environment, particularly through a network of gullies, leads to its proximity to the sampled wells.

The prevalence of polyphenols in these wells predominantly stems from the infiltration of water tainted by OMW from oil mills into the Innaouene River, subsequently polluting the groundwater.

Various factors contribute to the fluctuations in polyphenol levels detected in wells adjacent to oil mills:

- Water table depth concerning the ground level.
- Direction of groundwater flow.
- Number, operational processes, and size of nearby oil mills.
- Composition of the evaporation and OMW storage basins: For instance, if these basins are constructed from cement or prevent direct OMW spreading onto the ground, groundwater infiltration remains minimal. Conversely, porous materials or direct spreading can lead to substantial infiltration.

Proximity of the wells to the oil mills.

4. Conclusions

These factors collectively influence and account for the observed variations in polyphenol levels in wells adjacent to oil mills. The research conducted in this study contributes significantly from a physicochemical and hydrogeological standpoint to understanding the ramifications of wastewater from oil mills (OMW) on groundwater resources within the Oued Amlil region of the Taza province. The rapid growth of olive oil production, unfortunately, comes at the expense of the environment, especially concerning the discharge of untreated OMW into the natural surroundings. The susceptibility of groundwater to pollution is heightened due to the permeability of the subsoil, coupled with the relatively shallow water table rarely exceeding 35 meters. Various olive oil extraction methods, whether traditional, semi-modern, or modern, along with the exposure of OMW to evaporation in non-watertight basins, facilitate the infiltration of pollutants into the soil, leading to groundwater contamination. These OMW, rich in organic acids, significantly alter the water table's acidity, reduce dissolved oxygen content, and increase organic compound concentrations, notably polyphenols. The study's outcomes emphasize the pressing need for ecologically viable solutions to halt well contamination in the region. It's imperative to explore approaches that are both environmentally effective and practical to mitigate the impact of OMW on groundwater resources in the Taza province.

References

[1] L.A.S. Cavaca, I.M. López-Coca, G. Silvero & C.A.M. Afonso (2020). The olive-tree leaves as a source of high-added value molecules: Oleuropein, in: Studies in Natural Products Chemistry. 64:131–180. https://doi.org/10.1016/B978-0-12-817903-1.00005-X.

[2] A. Chiou & N. Kalogeropoulos (2017). Virgin Olive Oil as Frying Oil. Comprehensive Reviews in Food Science and Food Safety. 16(4):632–646. https://doi.org/10.1111/1541-4337.12268.

[3] V. Kinigopoulou, E. Hatzigiannakis, A. Guitonas, E.K. Oikonomou & P. Samaras (2023). Utilization of biobed for the efficient treatment of olive oil mill wastewat. Desalination and Water Treat. 223:167–179. https://doi.org/10.5004/dwt.2021.27123.

[4] B.M. Sidi, M. Ben, H.M. Sidi, R.K. Sidi, E. Kassioui & J. Sidi (2023). Assessment of the impacts of the meteorological drought on the Livestock Sector in the Province of Taza. Bulgarian Journal of Agricultural Science. 29(5):792-799.

[5] K. Haddad, M. Jeguirim, B. Jerbi, A. Chouchene, P. Dutournié, N. Thevenin, L. Ruidavets, S. Jellali & L. Limousy (2017). Olive Mill Wastewater: From a Pollutant to Green Fuels, Agricultural Water Source and Biofertilizer. ACS Publications. 5(10):8988–

8996.
https://doi.org/10.1021/acssuschemeng.7b01786.

[6] A. Yaakoubi & B. Aghanchich (2021). L'effet des margines sur la germination des graines de fève (Vicia faba. L). Afrique SCIENCE. 18(2):124-133. http://www.afriquescience.net.

[7] F. Cuomo, F. Venditti, G. Cinelli, A. Ceglie & F. Lopez (2016). Olive mill wastewater (OMW) phenol compounds degradation by means of a visible light activated titanium dioxide-based photocatalyst. Zeitschrift Fur Physikalische Chemie. 230(9):1269-1280. https://doi.org/10.1515/zpch-2015-0725.

[8] M. El Yamani, E.H. Sakar, A. Boussakouran, N. Ghabbour & Y. Rharrabti (2020). Physicochemical and microbiological characterization of olive mill wastewater (OMW) from different regions of northern Morocco. Environmental Technology. 41(23):3081-3093.
https://doi.org/10.1080/09593330.2019.1597926.

[9] N. Azbar, A. Bayram, A. Filibeli, A. Muezzinoglu, F. Sengul & A. Ozer (2004). A review of waste management options in olive oil production. Critical Reviews In Environmental Science and Technology. 34(3):209-247.
https://doi.org/10.1080/10643380490279932.

[10] A. Khdair & G. Abu-Rumman (2020). Sustainable environmental management and valorization options for olive mill byproducts in the Middle East and North Africa (MENA) region. Processes. 8(6):671. https://doi.org/10.3390/PR8060671.

[11] G. Ducom, M. Gautier, M. Pietraccini, J.P. Tagutchou, D. Lebouil & R. Gourdon (2020). Comparative analyses of three olive mill solid residues from different countries and processes for energy recovery by gasification. Renewable Energy. 145:180–189.
https://doi.org/10.1016/j.renene.2019.05.116.

[12] H. Aiman, Y. El Khalki, H. Reddad, J. Gartet & M. Abahrour (2021). COMPARAISON DES RESULTATS DE L'APPROCHE PAP/CAR ET LE MODELE USLE DANS LA CARTOGRAPHIE ET L'ESTIMATION QUALITATIVE DE L'EROSION HYDRIQUE DANS LE BASSIN VERSANT DE L'OUED AMLIL, (PRERIF - MAROC). Papeles de Geografía. 66:138-150. https://doi.org/10.6018/geografia.415511.

[13] A. Adjagodo, M. Agassounon Djikpo Tchibozo, N.C. Kelome & R. Lawani (2016). Flux des polluants liés aux activités anthropiques, risques sur les ressources en eau de surface et la chaine trophique à travers le monde : synthèse bibliographique. International Journal of Biological and Chemical Sciences. 10(3):1459. https://doi.org/10.4314/ijbcs.v10i3.43.

[14] O. Fassi-Fihri (1997). Etude hydrogéologique de l'aquifère liasique du couloir Fès-Taza (Maroc), IAHS Publ. 247.

[15] K. Belhassan, M.A. Hessane & A. Essahlaoui (2010). Interactions eaux de surface-eaux souterraines: Bassin versant de l'oued mikkes (maroc). Hydrological Sciences Journal. 55(8):1371–1384.
https://doi.org/10.1080/02626667.2010.528763.

[16] A. Ait Addi & D. Chafiki (2013). Sedimentary evolution and palaeogeography of mid-Jurassic deposits of the Central High Atlas, Morocco. Journal of African Earth Sciences. 84(12):54–69. https://doi.org/10.1016/j.jafrearsci.2013.04.002.

[17] S. Bahroun, H. Bousnoubra, N. Drouiche & N. Kherici (2016). Analysis of wastewater discharges to the Wadi Kebir East River by the environmental discharge objectives (EDO) method. Desalination and Water Treatment 57(52):1-5. https://doi.org/10.1080/19443994.2016.1146924.

[18] E. De Marco, M. Savarese, A. Paduano & R. Sacchi (2007). Characterization and fractionation of phenolic compounds extracted from olive oil mill wastewaters. Food Chemistry 104(2):858-867. https://doi.org/10.1016/j.foodchem.2006.10.005.

[19] I. Fki, N. Allouche & S. Sayadi (2005). The use of polyphenolic extract, purified hydroxytyrosol and 3,4-dihydroxyphenyl acetic acid from olive mill wastewater for the stabilization of refined oils: A potential alternative to synthetic antioxidants. Food Chemistry 93(2):197-204. https://doi.org/10.1016/j.foodchem.2004.09.014.

[20] V.L. Singleton, R. Orthofer & R.M. Lamuela-Raventos (1999). [14] Analysis of Total Phenols and Other Oxidation Substrates and Antioxidants by Means of Folin-Ciocalteu Reagent. Methods in Enzymology. 299:152-178.
https://doi.org/10.1016/S0076-6879(99)99017-1

[21] E. Portes, C. Gardrat & A. Castellan (2007). A comparative study on the antioxidant properties of tetrahydrocurcuminoids and curcuminoids. ChemInform. 38(50). https://doi.org/10.1002/chin.200750107

[22] B. Zghari, P. Doumenq, A. Romane & A. Boukir (2017). GC-MS, FTIR and 1 H , 13 C NMR Structural Analysis and Identification of Phenolic Compounds in Olive Mill Wastewater Extracted from Oued Oussefrou Effluent (Beni Mellal-Morocco). Journal of Materials and Environmental Sciences 8(12):4496-4509. 10.26872/jmes.2017.8.12.475

[23] M. Khellou, A. Laifa, M. Loudiki & M. Douma (2018). Assessment of phytoplankton diversity in two lakes from the northeastern Algerian sahara. Applied Ecology and Environmental Research. 16(3):3407-3419.
https://doi.org/10.15666/aeer/1603_34073419.

[24] G. Dunn, K. Bakker & L. Harris (2014). Drinking Water Quality Guidelines across Canadian provinces and territories: Jurisdictional variation in the context of decentralized water governance. International Journal of Environmental Research and Public Health. 11(5):4634-51. https://doi.org/10.3390/ijerph110504634.

[25] Y.F. Kouame, A.B.B. Kedi, S.S. Kouassi, N.J.A. Konan, E.S. Assohoun, O.B. Yapo & T. Gnagne (2021). Physicochemical characteristic of ground water for domestic use in the town of Daloa (Midwest, Ivory Coast). International Journal of

Biological and Chemical Sciences. 15:835–845. https://doi.org/10.4314/ijbcs.v15i2.33.

[26] J. Yuan, F. Xu, G. Deng, Y. Tang & P. Li (2017). Hydrogeochemistry of shallow groundwater in a karst aquifer aystem of Bijie City, Guizhou Province. Water 9(8):625. https://doi.org/10.3390/w9080625.